Fusion of Statistical Reasoning for Healing Highly Corrupted Image

Golam Moktader Daiyan[1]
School of Computer Science and Engineering
Digital Media Technology Key Laboratory of Sichuan Province
University of Electronic Science and Technology of China

Leiting Chen[2]
School of Computer Science and Engineering
Digital Media Technology Key Laboratory of Sichuan Province
University of Electronic Science and Technology of China
Institute of Electronics and Information Engineering in Guangdong, University of Electronic Science and Technology of China

Chuan Zho[3]*
School of Computer Science and Engineering
University of Electronic Science and Technology of China
Digital Media Technology Key Laboratory of Sichuan Province, University of Electronic Science and Technology of China
Institute of Electronics and Information Engineering in Guangdong, University of Electronic Science and Technology of China

Golam Moktader Nayeem[4]
School of Computer Science and Engineering
University of Electronic Science and Technology of China

***Abstract*—The accurate approximation of pixel value for preserving image details at a high concentration of noise has led the researchers to improve filters performance. A few image restoration filters are effective at lower density noise. Filters are commonly deployed for cameras, image processing tasks, medical image analysis, guided media data transmission, and real-time machine learning. This article proposes a mathematical model for the exact pixel value estimation at a high noise density for RGB and Gray images. The mathematical model is implemented to fuse statistical reasoning on the optimized mask sizes while preserving image details. Different parameter returns from the median filter, the trimmed median filter, the trimmed mean filter, and mood analysis form a mathematical function. The filter iteratively selects different schemes to calculate pixel values at different noise densities with minimum image information. Different processing masks are analyzed to preserve local data at specific image locations correctly in high density. A robust estimator counts false approximation of pixel values as discontinued, identified, and removed. At the post smoothening process, the filter recovers the misclassification of noise-free pixel and blur effects in the image. The qualitative experiments show satisfactory results in storing the details of the image from any image. The performance of the fusion filter is verified with visual quality and performance analysis matrices such as the image enhancement factor, the similarity indicator and the noise ratio from the peak signal.**

***Keywords*—Salt and pepper noise; median filter; statistical reasoning; performance analysis matrices; high-density noise; mood; trimmed median; trimmed mean; peak signal-to-noise ratio; image enhancement factor; structural similarity index**

I. INTRODUCTION

Some notable developments have attracted attention from the image processing industry to academia. Its research opportunities have been expanded due to the implementation of real-time applications in computer vision, digital image acquisition, satellite image analysis, data transmission and medical image analysis [1]. Preprocessing a digital image for a real-time application is essential before deploying for any application. This article focuses on significant preprocessing work and recommends a statistics-based mathematical model to eliminate digital images' salt and pepper noise (SAPN). The previously proven filters have been discussed here: standard median filter (SMF)[2], an adaptive median filter (AMF) [3], decision-based filter (DBA) [4], and noise-adaptive fuzzy switching median filter (NAFSM)[5]. The most common disadvantage of denoising is that the image information is lost in higher noise density [6].

SMF has a fundamental mathematical structure and displays the best output on low-density noise removal [7]. A mask with a 3X3 size limits the processing ability to select noise-free pixels at high densities. Nevertheless, several recent additions to nonlinear filters have outgrown existing filter errors and reached a stage where they may be suitable for approved types of noise. Nonlinear methods such as trimmed media filters, noise adaptive fuzzy median filters [5], decision-based median filters [4] have become the norm for image analysis.

Related research indicates that the development of the filtering phase is gradual, and the opportunity motivates the researcher to strengthen the filters based on statistical reasoning. This article investigates the fusion of statistical logic to design an effective filter to remove noise from the highly damaged image.

Filters are loosely classified according to their ability to reduce the noise of any concentration: when retrieved, images begin to have jitter effects, noise type, recovery of image data, image type, and noise removal from pure black and white dot [8]. The adaptive median filter mask shows a different technique for selecting a noise-free pixel by extending the size

*Corresponding Author

of 2 × 2 but fails due to limited statistical analysis and displacement of the denoised pixels at high noise densities. The adaptive median filter fails to store local information properly, while the noise adaptive fuzzy switching median filter [9](NAFSM)[10] and the decision-based filter (DBA) [4] repeatedly replace the noisy pixels that are resulting blurred effect on the restored images. However, the output of any filter can be improved to a certain extent by giving more weight to a particular pixel based on the surrounding pixel intensity statistics [11][12][9] [13].

Statistical analysis for the improvements of AMF, DBA, NAFSM, and other filters was initiated. However, a proper mathematical model is not yet proposed. Instead, most researchers have suggested multiple-combined filters to eliminate high-density pulse noise from the grey and colour images, regardless of the image's black and white part, discussed in Section 2.3. And most of them are not defined as state-of-the-art filters, such as morphological-mean filter [14], decision-based asymmetric filter (DBUF) [15] and filter boundary discriminative noise detection [16]. Most of the improved filters have the following drawbacks:

1) Most advanced/hybrid filters replace noise pixels under certain predefined conditions. Eliminating high SAPN concentration confuses filters to replace noisy pixels.

2) Most recently improved decision-based filters use threshold concepts and retain high noise density (above 50% noise density) in the restoration process. A striking effect is included separately in the restored image. In comparison, such filters do not perform well in extracting features from the medical image.

3) Most sophisticated filters and derivatives of median-type filters repeatedly replace the noise pixels in recovered images, regardless of the pixels in the 3×3 Mask.

A fusion-based statistical model performs iterative analysis on the different processing mask sizes for statistical analysis for image retrieval with improved visual quality from high-density SAPN. The filter iteratively selects the different mask sizes and performs comparative analysis based on neighbours pixels information and the non-local pixels information at 11X11 Mask to understand the image texture. The proposed filter has the following distinctive features to overcome the limitations:

A. Optimization of Texture-based Accurate Pixel Classification

Misclassification of noise pixels at high densities is a significant limitation of most filters. Most recently enhanced hybrid filters such as decision-based filters, noise-adapted obscure medium filters, interpolation-based filters [17], morphological filters [18], inpainting-based filters [19] to classify noisy pixels at high noise density.

B. Optimization of Mask Sizes to Fuse Statistical Analysis into the Mathematical Model

A filtering mask plays a vital role in removing high-density noise from the image regardless of local information at high density. The image texture should be maintained from any shape of the processing mask when retrieving an image from corruption, and the mathematical model is inspired by proper image texture management. A recommended mask size is preferred from the recently proposed hybrid filters discussed in Section 2.3. Experiments already have identified the use of a 3×3 mask as the best filtering option for removing low noise levels (<30 % noise) [20]. However, there are no optimal rules for determining the size of a mask that can be applied to a noise concentration. The algorithm provides a statistical, mathematical model that can repeatedly use different shapes of the Mask according to the noise density.

C. Statistical Reasoning to Identify Image Texture

The pixel intensity of the edges is identical to the details of the SAPN, which assumes it as the noise feature instead of evaluating edge information. The concept of axis based statistical analysis [6] is used here for edge detection based on the horizontal and vertical resolution in the Mask. The filter utilizes a primary mask at low density to identify the edges and noise-free pixels. But at high-density, different mask shapes are used repeatedly to reconstruct the edges, noise-free pixels, and non-local image details from corruption to image details.

D. Need for the Fusion of Statistical Model

Statistical analysis provides high visual quality and high efficiency of quantitative measurement with other popular filters. The quantitative measurements are the structural similarity index (SSIM) [21], the image enhancement factor (IEF) and the peak signal-to-noise ratio (PSNR) [22].

It provides a systematic decision rule for selecting processing mask size based on noise density. The rule-driven model allows multiple filters to work in an iterative process to estimate pixel intensity.

The above features distinguish from other existing filers in terms of retrieving an image from low and high noise concentrations. The model can be applied at the image preprocessing stage for image preparation for any application.

The rest of the paper is fourfold: It gives an overview of related literature, provides complete implementation methods of the proposed algorithm, performance analysis, and conclusion.

II. Literature Review

A. Salt and Pepper Noise (SAPN)

Reconstruction of digital images from high-density salt and pepper sounds is induced by transmissions, faulty sensors, or analogue-to-digital converters. Noise is evenly distributed in the image where infected pixels are usually identical to their neighbours. A fixed number of pixels that change to 0 or 255 is found in the salt and pepper noise (SAPN).

B. SAPN Detection Criteria for Existing and Hybrid Filters

Algorithms such as Noise Adaptive Fuzzy Switching Media Filters, Decision-Based Algorithms, and Adaptive Media Filters are standard today, often showing noise on the pixel intensity rather than identifying the properties of the surrounding pixels. Thus, filters select 0 or 255 noise-free volumes as noise pixels, contributing to incorrect detection in the image. It affects the decision on the image recovered from the high noise in a severe case. A noisy image has the following features:

1) SAPN is evenly or randomly scattered and spread over distorted images with equal probability.

2) Noisy pixels are not distinguished from noise-free 0 or 255. Again, the pixel intensity in that vicinity can be 0 (or 255) in most cases.

3) The SAPN often distorts the black and white information in the grey or RGB images. The salt or pepper noise is assimilated in the image white or black detail and lost, respectively.

Problems with the above design are considered when improving the filter. But the use of weak statistical methods or multiple filters consistently provides a certain level of performance. Advanced logic-based mathematical models or machine learning methods can overcome current performance limitations. Fig. 1 provides a classification of filters based on noise concentration.

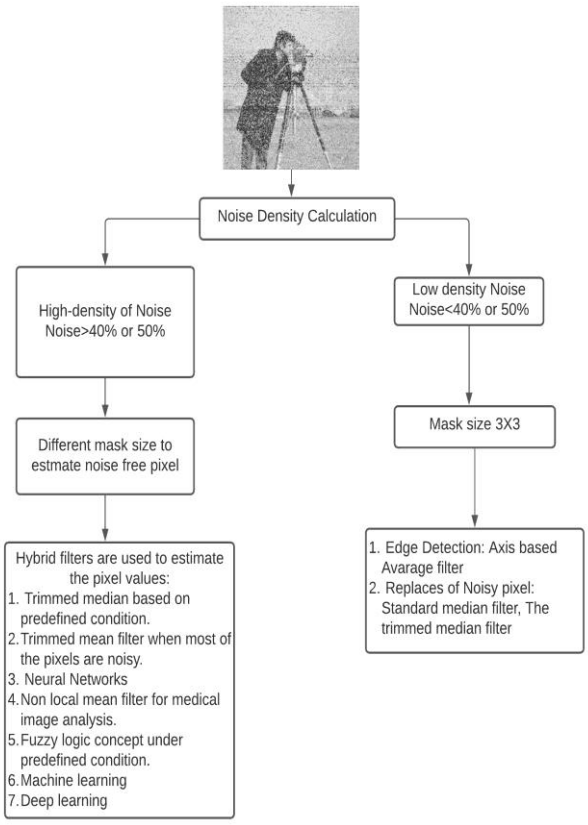

Fig. 1. Classification of Filters based on Noise Density.

C. Statistical or Mathematical Model used in Recently Published Journals

Recently published articles show that the most advanced filters are hybrid filter types, and a variety of filters act as a single algorithm applied to remove higher noise concentrations from images. The exact mathematical model for high-density pixel estimation has not yet been adequately defined. The statistical analysis of some recently published journals to identify trends in improving filters is summarized here in Table I. The table demonstrates the need to have an accurate mathematical model for eliminating noise at higher densities. Table I shows that filters for removing high-density noise are based on the systematic deployment of several filters in a single algorithm that improves the image quality at a certain level.

TABLE I. EXITING ALGORITHMS ACCURACIES

Filters	Statistical reasoning used for the filter design in recently published journals
The Axis-Based Filters[6]	The edges of the Mask are described with the aid of using a direct line passing via the primary pixel. Otherwise, its miles changed with the aid of using the expected value.
DBUTM Filter [23]	The mean of all four creaking neighbours replaces the noisy pels. If four neighbours aren't noisy, the corrupted pixel returns the unsymmetrical cut changed median value.
A CNN filter [24]	CNN model is used for denoising Salt and Pepper noise.
Modifed cascaded flter[8]	The trimmed median value replaces the noisy pixel while other pixel values, 0 and 255, are present at a high noise density in the selected window.
Improved Switching Median Filter [25]	The median value selection is based on the 2nd and 8th pixels of the 3 × 3, where all the pixels are arranged in a matrix in ascending order. Also, the window means is calculated from a 4X4 window.
Minimum-maximum median filter[26]	Selecting the mask size is entirely based on the noise density of the current processing window. Noisy pixel is replaced by the last processing pixel or median value.
Min-Max Filter[27]	Min-max average pooling is used here to remove SAPN noise.
Neural network[28]	The proposed algorithm utilizes a denoising convolutional neural network at a high noise density.
Tropical algebra-based adaptive filter[29]	The filter deployed tropical algebra to illustrate the adaptive principles to do away with salt and pepper noise.
A two-stage filter[30]	The filter behaves like a conventional filter; however, the high-density noisy pixel is changed using the median of the most repetitive pixels.
FFDNet: CNN based Image Denoising [34]	Proposed a CNN model.
Adaptive Algorithm and Wavelet Transform [33]	Utilizes Adaptive filering and Wavelet Transform

From Table I above, a summary of the most proposed hybrid filters between 2019 and 2021 can be summarized as follows:

1) The approximation of pixel intensity at high density is based on finding the noise-free pixel regardless of maintaining local features.

2) Install filters without comparing local information to different image properties at high density.

3) Sometimes pixel estimation relies on threshold value to estimate noisy pixels as noise-free.

4) Discontinuity of local pixels is not yet maintained at high density, which causes a blur effect in the image.

III. Methodology

In this section, a fusion of statistically based filters is presented, broadly divided into four subdivisions: the estimation of noise density, pre-edge filtering, and statistical reasoning based on ambient pixel intensity (the main algorithm of the filter), and post-smoothing filter (Robust Statistics). The block diagram of the proposed filter is demonstrated in Fig. 2.

A. Estimation of the Noise Density

The noise concentration of the processing mask is calculated to start the filtering process because it is an integral part of statistical analysis. Sound density (n_d)can be calculated using equations (1) and (2) [31].

$$Y_{(x,y)} = \begin{cases} 1, & q_{x,y} \in \{0,255) \\ 0, & \text{Otherwise} \end{cases} \quad (1)$$

$$N_d = \frac{\sum_{y=1}^{x=R} \sum_{y=1}^{x=C} Y_{x,y}}{R \times C} \times 100\% \quad (2)$$

Where, $q_{x,y}$ is the pixels of the noisy image, and R and C are the image dimension.

B. Filtration of the Edges of the Image Objects

At first, a 3X3 mask was taken to classify the contaminated pixels based on the horizontal and diagonal directions in the initial stage. If the pair of pixels in the horizontal or diagonal direction is the same, it is declared as the underlying processing pixel, $q_{x,y}$ Noise-free. The matching figure is shown in equation 3 below:

$$q(x,y) = \begin{cases} q_{x+1,y+1}, & \text{if, } q_{x+1,y+1} = q_{x-1,y-1} \\ q_{x+1,y-1} & \text{if, } q_{x+1,y-1} = q_{x-1,y+1} \\ q_{x,y+1,} & \text{if, } q_{x,y+1} = q_{x,y-1} \\ q_{x,y} & \text{Trimmed Median} \end{cases} \quad (3)$$

It can be seen that the original values replace most of the pixels recovered in this process, and here the incorrect classification of pixels is reduced in a high density of noise.

This technique is considered when enough noise-free pixels are available to detect edges in the processing mask. Otherwise, the trimmed medium filter is placed in the processing mask. The block diagram of the vertical and horizontal edge detection scheme is given in Fig. 3.

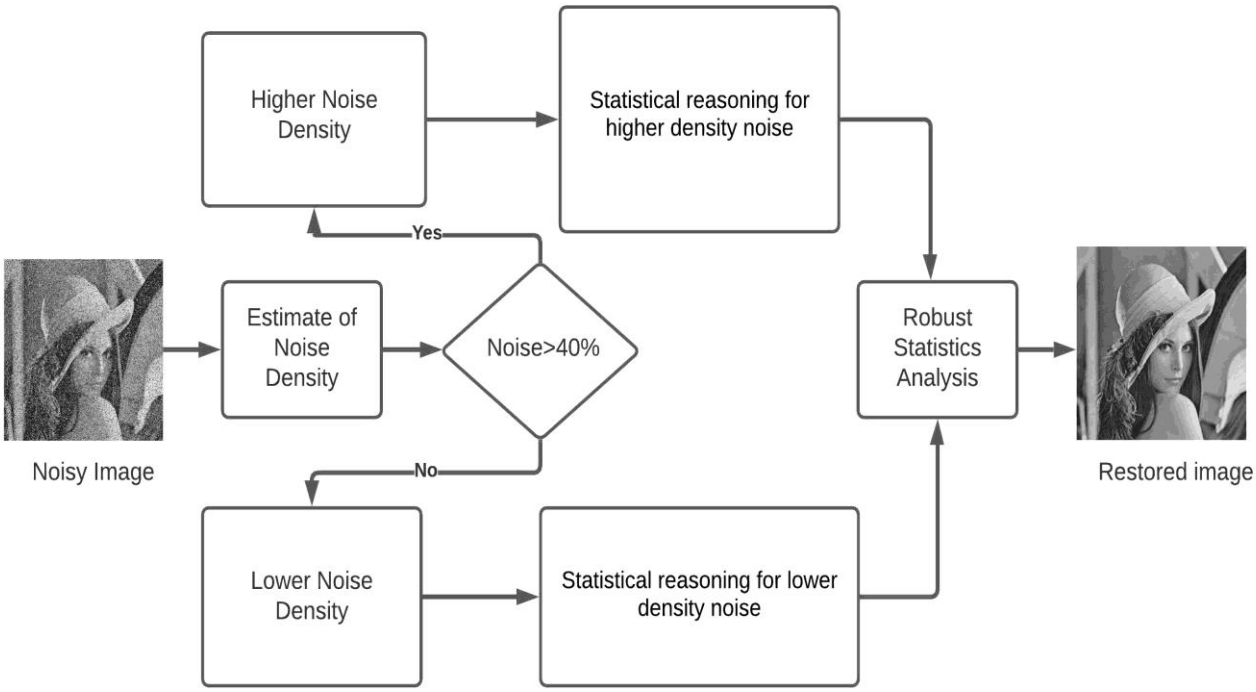

Fig. 2. Block Diagram of the Proposed Filter.

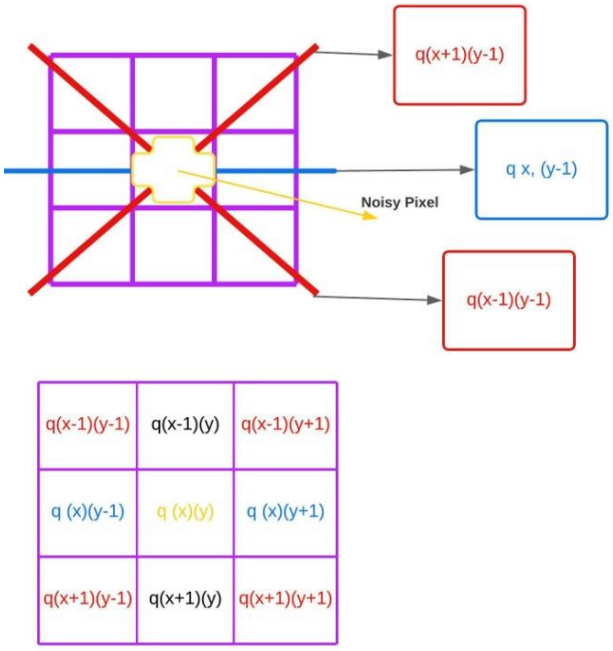

Fig. 3. Filtration of the Edges from the Image Objects.

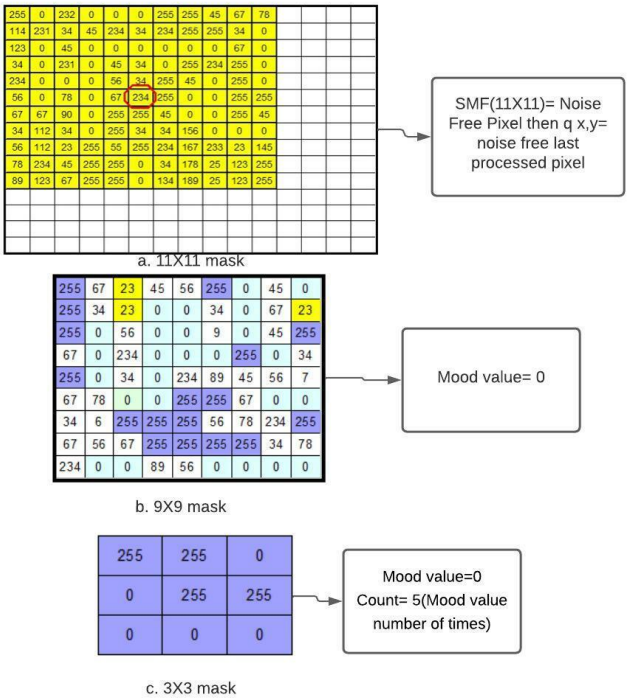

Fig. 4. Comparison Analysis on different Mask at Higher Density.

C. Statistical Reasoning based on Ambient Pixel Intensity

At higher noise concentrations, the filter utilizes 3X3, 9X9, and 11X11 masks, and at the lower noise <40% density, only a 3X3 mask is applicable to perform edge detection and noise elimination. The trimmed median value shows the best result after detecting edges at lower noise density. Mood value is estimated from the 11X11 Mask for the pure image black and white data. Statistical analysis from 3X3 and 9X9 masks offer a function to calculate the pixel intensity of distorted images as given in an equation (4).

$$U_{x,y} = (\propto\times\ q_{x-1,y-1}) + (1.0-\propto)\mathrm{SMF}(11\times 11) \quad (4)$$

Here,

$\propto = (\frac{mood(3\times 3\ mask)}{9})$,

$1 - q_{x,y} =$ *Last processed pixel* ,

$SMF(11\times 11) = Median\ value\ of\ 9\times 9$ Mask.

If the last processed pixel is, $q_{x-1,y-1} = 0\ or\ 255$, and all the pixels at 11×11 Mask is $0\ or\ 255$, then the filter detects this image detail is pure black or white. Then the complete statistical equation is shown in (5).

$$q_{x,y} = \begin{cases} U_{x,y}, & \text{if } 1 - q_{x,y} \neq 0 \text{ or } 255,\ \ \text{Noise} > 40\% \\ \text{Mood}(9\times 9), & \text{Otherwise} \end{cases} \quad (5)$$

Tests show that PSNR values drop sharply when $N_d >$ 40%. Statistical analysis of decision-making is based on the SAPN density of the Mask is considered here. Fig. 4 shows the different mask size sizes required to estimate intensity value. The proposed filter iteratively use the filter and perform median, mood and probability analysis on image data.

The need to select both masks of 9X9 and 11X11 is shown in a, b, and c of Fig. 5. The size of the Mask above 11X11 could not properly store local information. Thus, the statistical analysis is entirely dependent on 3 × 3, 9 × 9, and 11 × 11 masks. Experiment shows that, filter with size more than11 × 11 could not maintain the local image information at high density of noise. Fig. 5 visually demonstrates the trimmed median and the mood at e and f.

1) Post-smoothing filter: A smooth step has been added to the algorithm to improve the image quality further. The Robust Estimation is based on the principle that safety is more important than efficiency[32]. Here, the median is an estimator. Let q^1, q^2, q^3 ----- q^n indicate a random pixel from that processing image.

Algorithm 1(Removal of higher density SAPN):

$q_{x,y} \leftarrow Input\ \ Noisy\ image$
if $N_d < 40$ && $M_{3\times 3}$
{ *if* $Q_{xy} \leftarrow q(x,y)$ // Filtration of the edges
else
$Q_{xy} \leftarrow M_t(q_{x,y})$ // Trimmed Median
}
elseif $N_d > 40$ && $(1 - q_{x,y}) \neq 0 \,||\, 255$ && $M_{9\times 9}$
$Q_{xy} \leftarrow U_{x,y}$
else $N_d = 100$ && $M_{9\times 9}$
$Q_{xy} \leftarrow Mood(q_{x,y})$
Algorithm2 $\leftarrow Q_{xy}$

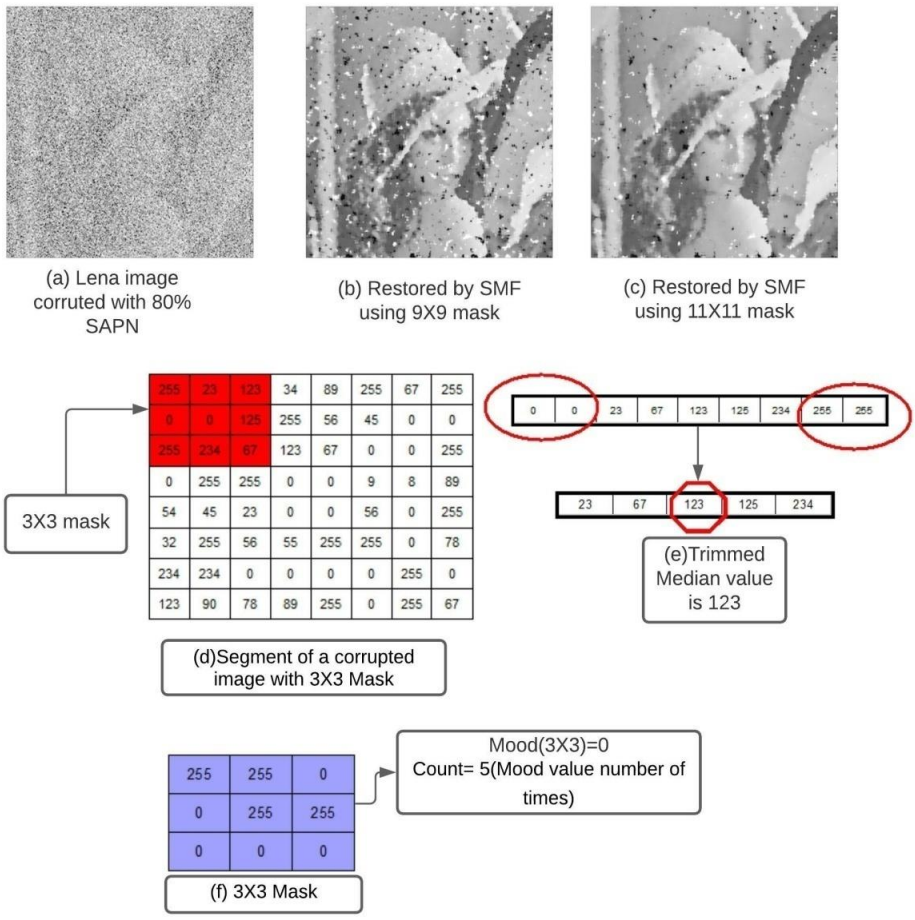

Fig. 5. Statistical Reasoning: (a) Lena Image Corrupted with 80% SAPN (b) Restored by SMF using 9 × 9 Mask (c) Restored by SMF using 11 × 11 Mask (d) the Segment of the Corrupted Image (e) the Trimmed Median (f) Mood Value.

U1 is the minor key of Qi, U2 is the following key in the sequence of Qi, and Un is the largest in the list (ascending order). The estimation of the new median, which removes pixel discontinuity in the image, is based on the L1 norm or Laplacian Distribution. The influence function is constant for the median, making the median an excellent and robust estimator. Robust Estimator is the M-estimators that are pretty good for distribution with outliers (scatter data value). The effects of robust estimators are compared in terms of influence function in the equation (6).

$$\varphi(q) = \begin{cases} 1 & q > 0 \\ -1 & q < 0 \end{cases} \quad (6)$$

Lorentz has an influence function of an estimator that tends to zero to increase the estimation distance and maximum value for the breakdown, which is used to the original pixel value from a corrupted image. The equations are given in (7) and (8).

$$P(q) = log\frac{(1+x^2)}{2\sigma^2} \quad (7)$$

$$\varphi = \frac{2q}{2\sigma^2+q} \quad (8)$$

Robust estimation is applied to minimize pixel discontinuity of the corrupted image, which eliminates blur effects from the image. The SAPN is first identified based on this method's minimum (0) and maximum (255) values. It is considered noise-free if the current pixel is within the dynamic range 0 and 255. Otherwise, it is seen as a noise pixel and is replaced by a value determined by the following algorithm using the Lorentzian Estimator.

Algorithm 2(Robust Statistics):

1: $Q_{x,y} \leftarrow Input\ preprocess\ image\ layer$
2: $if\ Q_{med} \leftarrow SAPN\ and\ Mask = 3 \times 3$
3: $P_{x,y} \leftarrow Q_{med} - Q_{xy}$
4: $if\ P_{x,y} \leftarrow SAPN$
//calculate the robust influence function
5: $\varphi(p) \leftarrow \frac{2p}{2\sigma^2+p^2}$
6: $s1 \leftarrow \sum_{l\in L} \frac{Pixel(l)\times\varphi(x)}{p}$
7: $s2 \leftarrow \sum_{l\in L} \frac{\varphi(x)}{p}$
//Estimated pixel value
8; $Q_{x,y} \leftarrow s1/s2;$
9: $R_{x,y} \leftarrow Restored\ image$

IV. RESULTS

The statistics model and popular filters are programmed in MATLAB 2014 and then simulated with the 14 benchmark images used in related journals to study filter performance. The evaluation task is to calculate a denoised image with a noise density in the medium to high range (40% to 90%). The denoised images are judged in terms of visual quality and performance analysis matrices.

A. Evaluating by Quantitative Comparison

The visual reports are taken from the simulation to judge the significance of the proposed filter in terms of visual quality. The famous benchmark data for image denoising are Fishing Boat, Baboon, Pepper, Barbara, Bubble, and Camera Man. The visual quality shows that SAPN can be extracted from any digital image by the proposed filter.

Fig. 6 to 11 visually compare the proposed filter and other existing filters. Benchmark datasets are corrupted with SAPN at different levels of noise concentration, and the same datasets are restored from the stated filters. Recovered images are visually compared, and it is seen that the proposed filter has the best performance in creating high-quality images. As in the case of Fig. 6 and 7, the images are restored from 70% and 90% of the SAPN where the images are visually compared to the proposed filter outperforms the other filters. The optimal suppression power at all levels of noise concentration is shown in Fig. 8 and 9. Furthermore, Fig. 10 shows that 50% of bubbles have been recovered from noise.

The proposed filter cannot correctly restore the image because some parts have too rough transitions. It should be noted that most sophisticated filters, such as SMF, AMF, DBA, and MDBUTMF, are weak in effectively detecting noise pixels when the noise pollution in the image is above 40%. The visual comparison shows that they often fail to classify the pixel as noise-free at higher noise density, causing a blurring effect on images. In this case, the proposed filter applied post smoothing statistical analysis to remove image artefacts and blurring effects. The proposed filter did not perform well in the bubble image of Fig. 8 but shows excellent performance in removing noise from the cameraman's images in Fig. 11. Fig. 6 to 11 visually compare the proposed filter and other existing filters. Benchmark datasets are corrupted with SAPN at different levels of noise concentration, and the same datasets are restored from the stated filters. Recovered images are visually compared, and it is seen that the proposed filter has the best performance in creating high-quality images. As in the case of Fig. 6 and 7, the images are restored from 70% and 90% of the SAPN where the images are visually compared to the proposed filter outperforms the other filters. The optimal suppression power at all levels of noise concentration is shown in Fig. 8 and 9. Furthermore, Fig. 10 shows that 50% of bubbles have been recovered from noise. The proposed filter cannot correctly restore the image because some parts have too rough transitions.

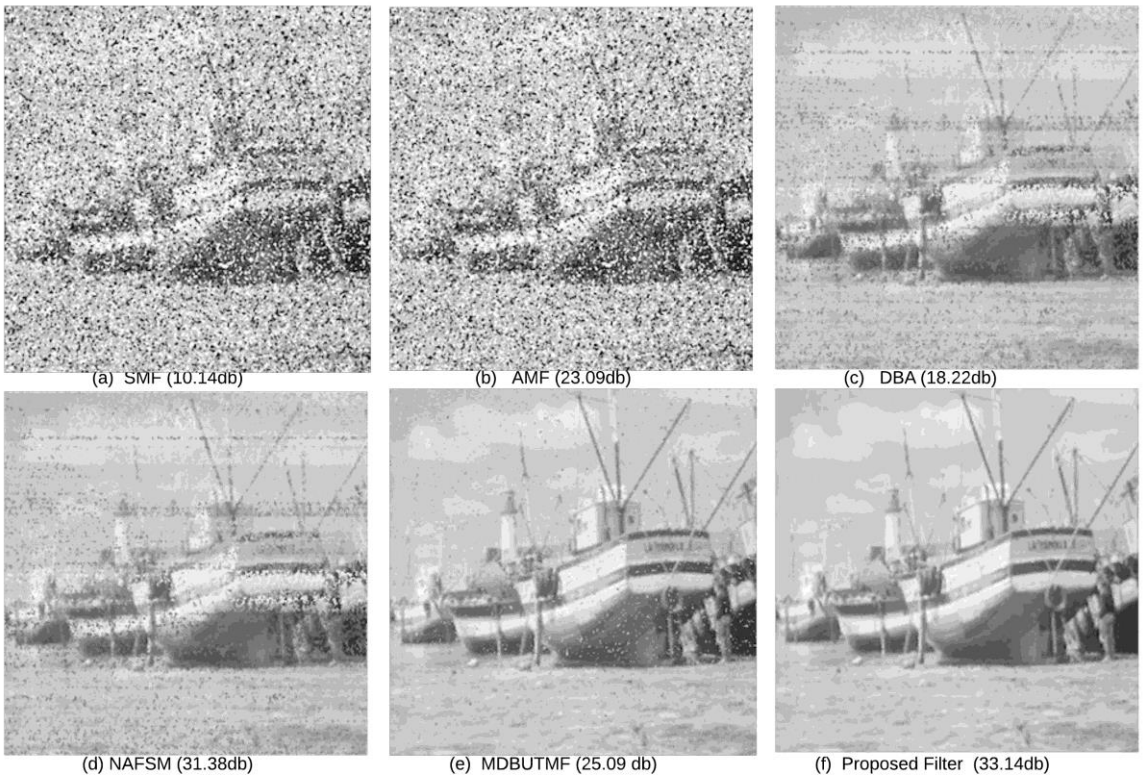

Fig. 6. (From Upper Left) a Fishing Boat Image Dnoised from 70% SAPN using ((a) SMF, (b) AMF, (c) DBA, (d) NAFSM Filter, (e) MDBUTMF and (f) PA.

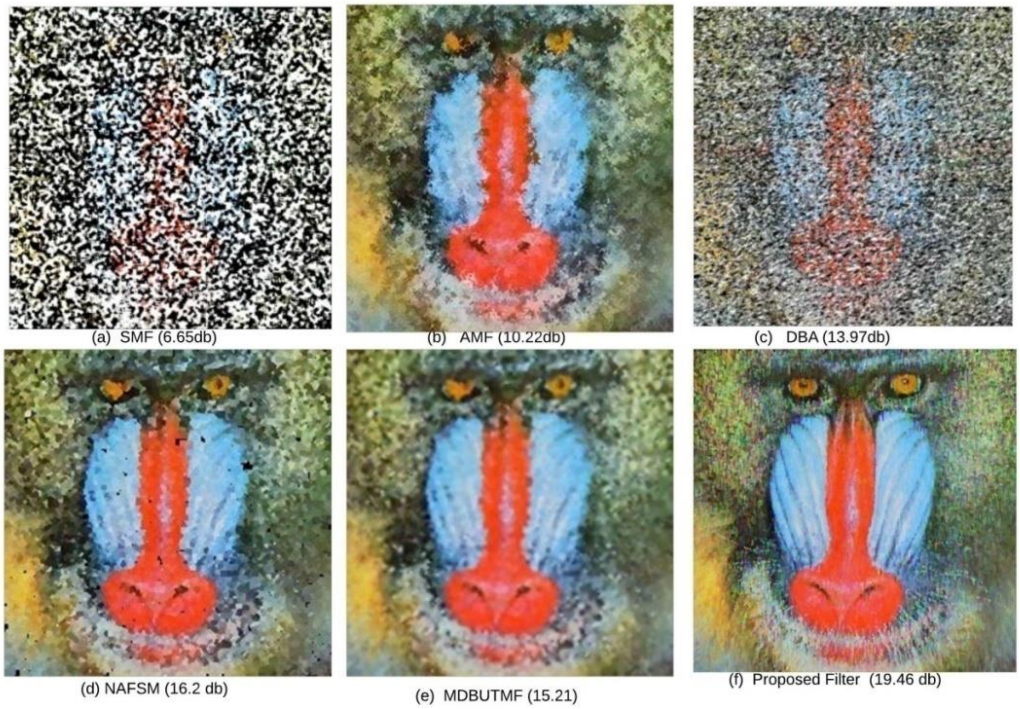

Fig. 7. (From Upper Left) Baboon Image Restored from 90% SAPN using ((a) SMF, (b) AMF, (c) DBA, (d) NAFSM Filter, (e) MDBUTMF and (f) PA.

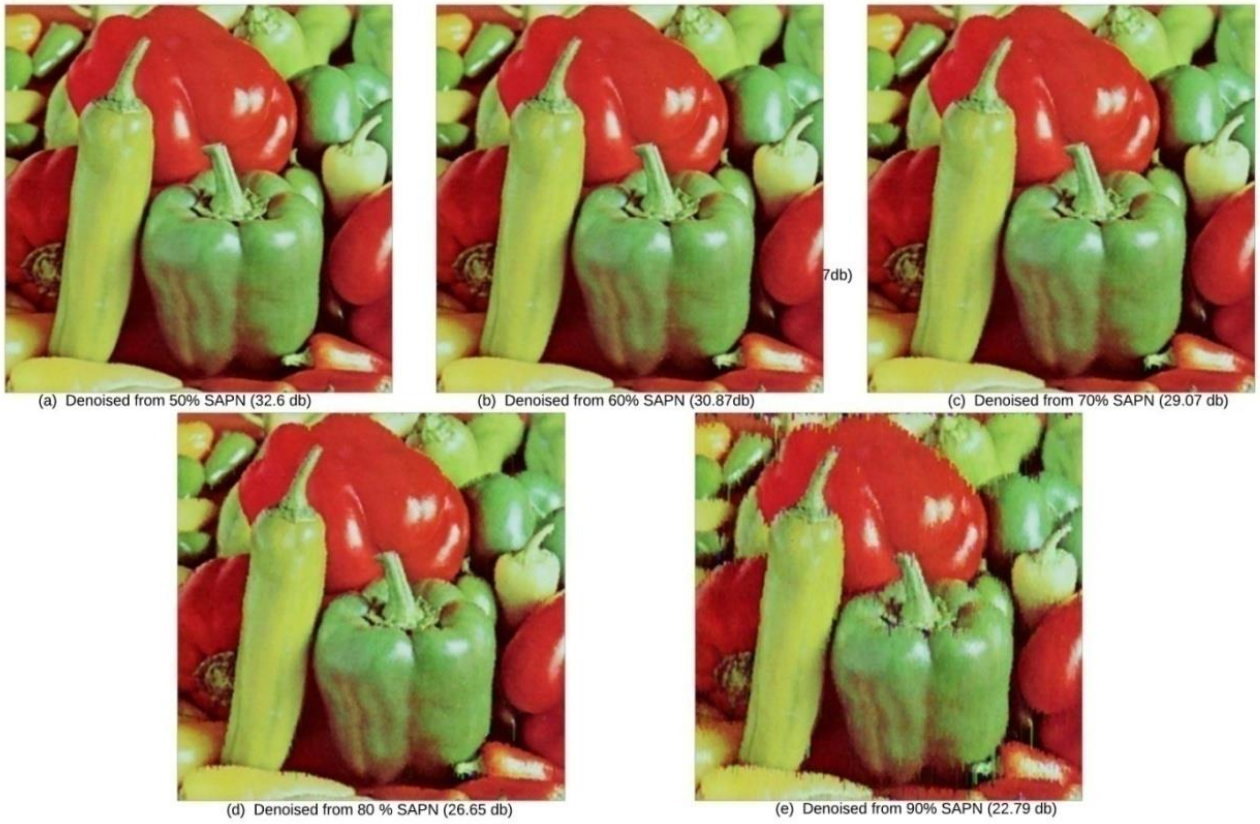

Fig. 8. (From Upper Left) Pepper Image Corrupted with 50% to 90% SAPN and Restored with PA.

Fig. 9. (From Upper Left) Barbara Image Corrupted with 50% to 90% SAPN and Restored with PA.

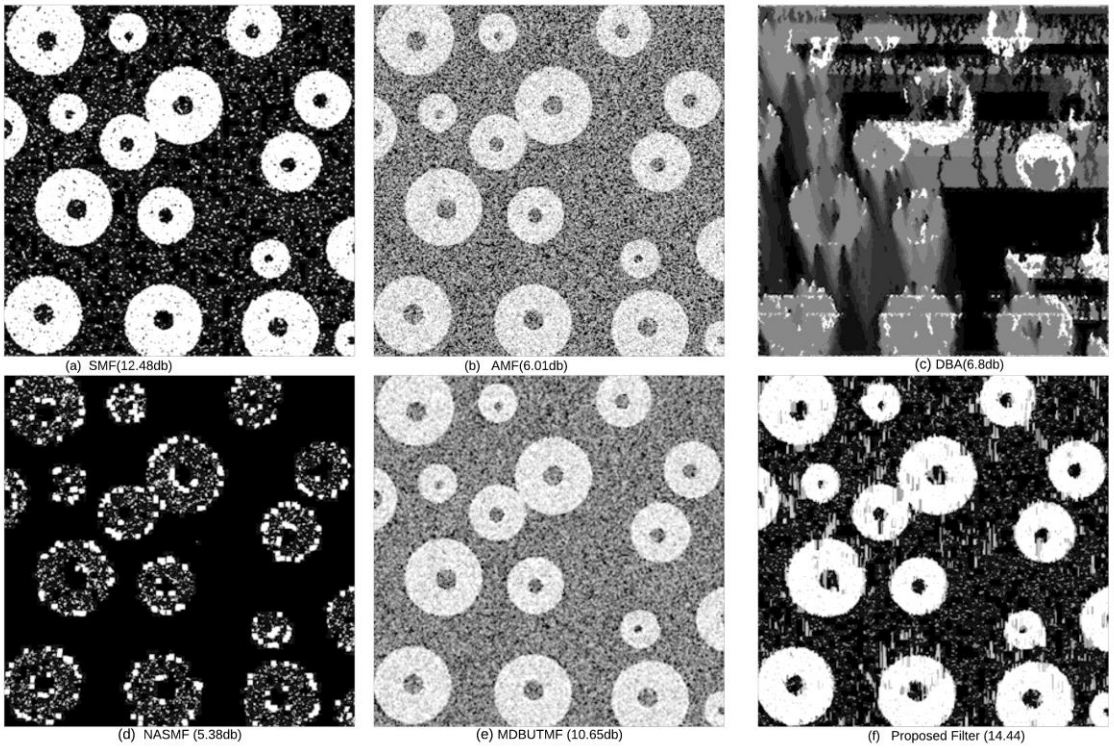

Fig. 10. (From Upper Left) Bubble Image Restored from 50% SAPN using (a) SMF, (b) AMF, (c) DBA, (d) NAFSM Filter, (e) MDBUTMF and (f) PA.

Fig. 11. (From Upper Left): Cameraman Image Denoised from 80% SAPN using (a) SMF, (b) AMF, (c) DBA (d) NAFSM Filter, (e) MDBUTMF, and (f) PA.

B. Evaluating by Quantitative Comparison

In this article, the Peak Signal-to-Noise Ratio (PSNR), Mean Square Error (MSE), Image Enhancement Factor (IEF), and Structural Similarity Index (SSIM) are considered for quantitative analysis. The PSNR is defined as the ratio between the original image's strength and the denoised image's strength, and the mathematical equation is given in (9).

$$\text{Peak Signal to Noise Ratio} = 10\log_{10}\frac{(MAX \times MAX)}{MSE} \quad (9)$$

Here , MAX is the maximum gray level of the image, and the Mean Square Error(MSE) is defined in the equation (10).

$$\text{Mean Square Error} = \frac{1}{RC}\sum(P_{x,y} - Q_{x,y})^2 \quad (10)$$

The R and C is the dimension of the image, $Q_{x,y}$ – original image and the $P_{x,y}$ - restored image. Another parameter is used, the Image Enhancement Factor (IEF). The mathematical expression of IEF is given in the equation (11).

$$\text{Image Enhancement Factor} = \frac{\sum_{i=1}^{M}\sum_{j=1}^{N}(N_{ij} - R_{ij})^2}{\sum_{i=1}^{M}\sum_{j=1}^{N}(X_{ij} - R_{ij})^2} \quad (11)$$

Where R_{ij} , X and N_{ij} denote the original image, denoised image, and corrupted image, respectively. The final parameter used to evaluate the proposed filter's performance is Structural Similarity Index. The mathematical expression is in an equation (12).

$$\text{SSIM}(x, y) = \frac{(2\mu_x\mu_y + c_1)(2\sigma_{x,y} + c_2)}{(\mu_x^2 + \mu_y^2 + c_1)(\sigma_x^2 + \sigma_y^2 + c_2)} \quad (12)$$

Here, μ_x and μ_y are the standard deviation used as an estimation of the signal contrast, σ_x and σ_y are the contrast comparison, and C1 and C2 are the constant value with a limit of 1.

C. Experimental Results of Tabular Style for High Density of Noise for Baboon(Grey) and Lena(RGB) Images

Tables II and III summarize the IEF, PSNR, and SSIM values for the six filters in the Baboon Grayscale and Lena RGB images. The experimental clearly show that the proposed algorithm has the edge over reported filters. Sometimes the Proposed filter cannot deliver optimal results in specific embodiments if certain image parts have very rough transitions or an utterly smooth area. Nevertheless, the average improvement of the proposed filter is the best from existing filters at SAPN density varies from 50% to 90%.

This, the performance of PSNR is exceptionally good for the noise concentration > 70%. Even at SAPN concentrations up to 95%, the proposed algorithm provides a fair average value compared with other existing filters. At medium noise concentrations, the effectiveness of NAFSM manages to surpass the Proposed algorithm but still exceeds existing strategies.

TABLE II. IEF, PSNR AND SSIM RESULTS ON THE BABOON.JPG FOR MEDIUM TO HIGH DENSITY

QA	Noise density	SMF	AMF	DBA	NAFSM	MDBUTMF	PA
IEF	50	3.96	23.96	12.49	30.94	24.19	39.33
	60	2.67	20.69	10.99	28.14	22.36	35.53
	70	1.9	15.32	9.34	25.16	18.57	30.55
	80	1.45	6.86	8.12	22.14	13.5	25.04
	90	1.18	2.68	6.36	16.81	8.44	19
PSNR	50	14.47	22.3	19.47	23.41	22.34	25.04
	60	11.96	20.85	18.1	22.19	21.19	23.89
	70	9.83	18.89	16.74	21.04	19.72	22.61
	80	8.05	14.81	15.54	19.9	17.75	21.19
	90	6.65	10.22	13.97	18.2	15.21	19.46
SSIM	50	0.21	0.69	0.49	0.74	0.69	0.86
	60	0.11	0.59	0.38	0.66	0.6	0.79
	70	0.06	0.46	0.28	0.57	0.48	0.69
	80	0.03	0.24	0.18	0.46	0.32	0.56
	90	0.01	0.06	0.09	0.29	0.16	0.39

TABLE III. IEF, PSNR AND SSIM RESULTS ON THE LENA.JPG FOR MEDIUM TO HIGH DENSITY

QA	Noise density	SMF	AMF	DBA	NAFSM	MDBUTMF	PA
IEF	50	4.9	145.35	18.63	261.33	138.33	387.83
	60	2.99	95.82	14.03	210.52	95.48	288.92
	70	2.02	34.39	10.98	176.14	50.04	224.04
	80	1.49	9.9	8.3	128.92	21.7	147.05
	90	1.19	2.94	6.18	62.23	9.14	79.96
PSNR	50	15.25	29.97	21.05	32.52	29.76	33.41
	60	12.31	27.37	19.02	30.79	27.35	31.78
	70	9.92	22.24	17.28	29.34	23.87	30.14
	80	8.02	16.25	15.49	27.4	19.66	27.79
	90	6.52	10.46	13.68	23.72	15.39	24.22
SSIM	50	0.16	0.75	0.4	0.8	0.72	0.92
	60	0.07	0.66	0.3	0.74	0.61	0.86
	70	0.03	0.49	0.22	0.66	0.43	0.78
	80	0.02	0.24	0.15	0.56	0.23	0.68
	90	0.01	0.04	0.08	0.39	0.09	0.51

D. Experimental Results of Graphical Style for Low Noise Concentration for Pepper Image

The performance of the proposed algorithm is tested with a pepper image, and the noise density varies from 10% to 40%. Restoration performance is quantitatively measured by metrics such as IEF, PSNR and SSIM, as shown in Fig. 12, 13 and 14. The SMF replaces the processing pixel by its median regardless of the type of pixel, which provides poor performance. However, the AMF [8] shows improved performance, but the loss of local image details is much more significant due to its adaptive nature. Predefined condition-based filters such as NAFSM and decision-based filters failed to retrieve images correctly.

The trimmed median filter always considers median values from the processing mask eliminating 0 and 255, which failed to store image edges and local information properly. Necessary features that may supressed noise for filters should also be taken care of for image processing tasks. The mathematical model also focused on this described in low density. Tests show that the exact pixel estimate of the proposed filters in low-density noise is the highest of the popular filters.

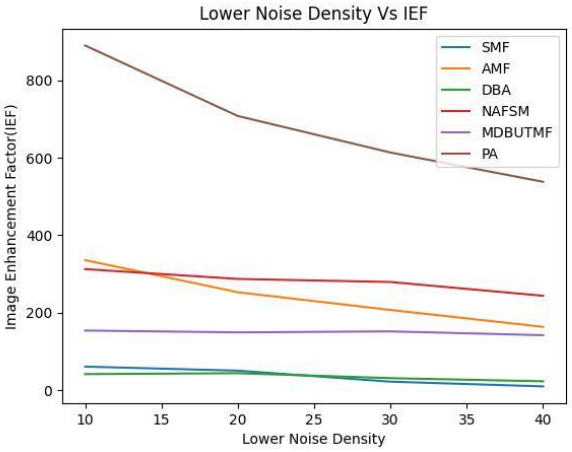

Fig. 12. Quantitative Analysis of Filters using IEF for Pepper Image.

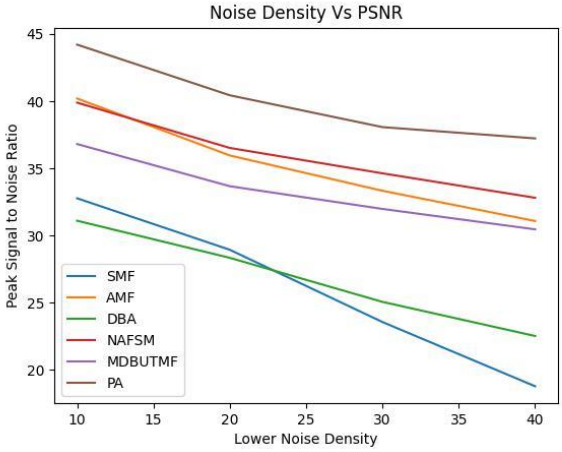

Fig. 13. Quantitative Analysis of Filters using PSNR for Pepper Image.

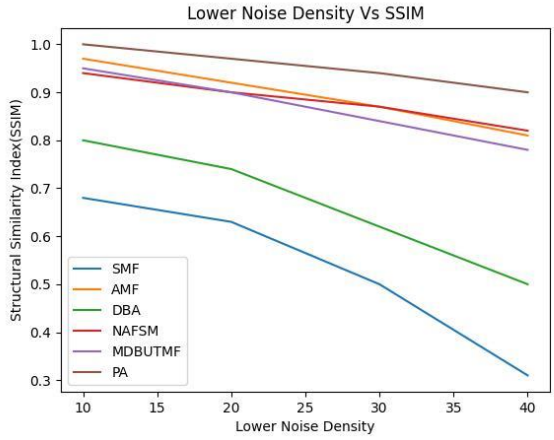

Fig. 14. Quantitative Analysis of Filters using SSIM for Pepper Image.

V. Conclusion

In this article, a complete and relative study of some sophisticated filters evaluates their performance in high-density noise removal. A fusion filter has been developed to deal with high-density noise. Statistical analysis was conducted on high-density noise, pixel estimation, data saving, white and black data identification of images, and removal of isolated pixels for data discontinuity without normalizing the image intensity. The proposed model provides the best results for noise removal at any concentration level. The main drawback of this filter is that the streaking effect occurs only when the high concentration of noise is removed from the pure black and white or medical images. Incorporating non-local statistical concepts into the proposed mathematical model could eliminate the streaking effect when removing high-density noise from medical images. The proposed algorithm can be placed on any digital devices as an image preprocessor.

References

[1] H. Liang, N. Li, and S. Zhao, "Salt and pepper noise removal method based on a detail-aware filter," Symmetry (Basel)., vol. 13, no. 3, 2021, doi: 10.3390/sym13030515.

[2] R. C. González, R. E. Woods, and S. L. Eddins, Digital Image Processing Using MARLAB. Pearson, 2004.

[3] H. Hwang and R. A. Haddad, "Adaptive median filters: new algorithms and results," IEEE Trans. image Process., vol. 4, no. 4, pp. 499–502, 1995.

[4] K. S. Srinivasan and D. Ebenezer, "A new fast and efficient decision-based algorithm for removal of high-density impulse noises," IEEE Signal Process. Lett., vol. 14, no. 3, pp. 189–192, 2007.

[5] K. K. V. Toh and N. A. M. Isa, "Noise adaptive fuzzy switching median filter for salt-and-pepper noise reduction," IEEE Signal Process. Lett., vol. 17, no. 3, pp. 281–284, 2009.

[6] A. Kundu, S. Banerje, C. Sarkar, and S. Barman, "An Axis Based Mean Filter for Removing High-Intensity Salt and Pepper Noise," 2020 IEEE Calcutta Conf. CALCON 2020 - Proc., vol. 1, pp. 363–367, 2020, doi: 10.1109/CALCON49167.2020.9106561.

[7] Z. Shen, J. Ni, and C. Chen, "Blind detection of median filtering using linear and nonlinear descriptors," Multimed. Tools Appl., vol. 75, no. 4, pp. 2327–2346, 2016.

[8] B. Karthik, T. Krishna Kumar, S. P. Vijayaragavan, and M. Sriram, "Removal of high density salt and pepper noise in color image through modified cascaded filter," J. Ambient Intell. Humaniz. Comput., vol. 12, no. 3, pp. 3901–3908, 2021, doi: 10.1007/s12652-020-01737-1.

[9] K. Ramamoorthy, T. Chelladurai, and P. N. Sundararajan, "Edge analysis for noise suppression in ultrasound kidney images using weighted median filter," Int. J. Syst. Signal Control Eng. Appl., vol. 7, no. 2, pp. 36–42, 2014.

[10] V. Jayaraj and D. Ebenezer, "A new switching-based median filtering scheme and algorithm for removal of high-density salt and pepper noise in images," EURASIP J. Adv. Signal Process., vol. 2010, no. 1, p. 690218, 2010.

[11] G. Balasubramanian, A. Chilambuchelvan, S. Vijayan, and G. Gowrison, "An extremely fast adaptive high-performance filter to remove salt and pepper noise using overlapping medians in images," Imaging Sci. J., vol. 64, no. 5, pp. 241–252, 2016.

[12] N. Singh, T. Thilagavathy, R. T. Lakshmipriya, and O. Umamaheswari, "Some studies on detection and filtering algorithms for the removal of random valued impulse noise," IET Image Process., vol. 11, no. 11, pp. 953–963, 2017.

[13] H. C. Bandala-Hernandez et al., "Weighted median filters: An analog implementation," Integration, vol. 55, pp. 227–231, 2016.

[14] R. Kunsoth and M. Biswas, "Modified decision based median filter for impulse noise removal," in 2016 International Conference on Wireless Communications, Signal Processing and Networking (WiSPNET), 2016, pp. 1316–1319.

[15] D. Shekar and R. Srikanth, "Removal of High Density Salt \& Pepper Noise in Noisy Images Using Decision Based UnSymmetric Trimmed Median Filter (DBUTM)," Int. J. Comput. Trends Technol., vol. 2, no. 1, pp. 109–114, 2011.

[16] P.-E. Ng and K.-K. Ma, "A switching median filter with boundary discriminative noise detection for extremely corrupted images," IEEE Trans. image Process., vol. 15, no. 6, pp. 1506–1516, 2006.

[17] C. Kalyoncu, Ö. Toygar, and H. Demirel, "Interpolation-based impulse noise removal," IET Image Process., vol. 7, no. 8, pp. 777–785, 2013.

[18] M. Gonzalez-Hidalgo, S. Massanet, A. Mir, and D. Ruiz-Aguilera, "Improving salt and pepper noise removal using a fuzzy mathematical morphology-based filter," Appl. Soft Comput., vol. 63, pp. 167–180, 2018.

[19] K. Gupta, N. Goyal, and H. Khatter, "Optimal reduction of noise in image processing using collaborative inpainting filtering with Pillar K-Mean clustering," Imaging Sci. J., vol. 67, no. 2, pp. 100–114, 2019, doi: 10.1080/13682199.2018.1560958.

[20] D. Guo, Z. Tu, J. Wang, M. Xiao, X. Du, and X. Qu, "Salt and Pepper Noise Removal with Multi-Class Dictionary Learning and L0 Norm Regularizations," Algorithms, vol. 12, no. 1, p. 7, 2019.

[21] U. Sara, M. Akter, and M. S. Uddin, "Image quality assessment through FSIM, SSIM, MSE and PSNR—A comparative study," J. Comput. Commun., vol. 7, no. 3, pp. 8–18, 2019.

[22] A. Tanchenko, "Visual-PSNR measure of image quality," J. Vis. Commun. Image Represent., vol. 25, no. 5, pp. 874–878, 2014.

[23] V. kishorebabu and R. Varatharajan, "A decision based unsymmetrical trimmed modified winsorized variants for the removal of high density salt and pepper noise in images and videos," Comput. Commun., vol. 154, pp. 433–441, 2020, doi: 10.1016/j.comcom.2020.02.048.

[24] B. Fu, X. Zhao, Y. Li, X. Wang, and Y. Ren, "A convolutional neural networks denoising approach for salt and pepper noise," Multimed. Tools Appl., vol. 78, no. 21, pp. 30707–30721, 2019, doi: 10.1007/s11042-018-6521-4.

[25] S. Anwar and G. Rajamohan, "Improved Image Enhancement Algorithms based on the Switching Median Filtering Technique," Arab. J. Sci. Eng., vol. 45, no. 12, pp. 11103–11114, 2020, doi: 10.1007/s13369-020-04983-9.

[26] B. Garg, "An adaptive minimum-maximum value-based weighted median filter for removing high density salt and pepper noise in medical images," Int. J. Ad Hoc Ubiquitous Comput., vol. 35, no. 2, pp. 96–116, 2020, doi: 10.1504/IJAHUC.2020.109795.

[27] P. Satti, N. Sharma, and B. Garg, "Min-Max Average Pooling Based Filter for Impulse Noise Removal," IEEE Signal Process. Lett., vol. 27, pp. 1475–1479, 2020, doi: 10.1109/LSP.2020.3016868.

[28] A. Noor, Y. Zhao, R. Khan, L. Wu, and F. Y. O. Abdalla, "Median filters combined with denoising convolutional neural network for Gaussian and impulse noises," Multimed. Tools Appl., vol. 79, no. 25–26, pp. 18553–18568, 2020, doi: 10.1007/s11042-020-08657-4.

[29] A. Abdurrazzaq, I. Mohd, A. K. Junoh, and Z. Yahya, "Tropical algebra based adaptive filter for noise removal in digital image," Multimed. Tools Appl., vol. 79, no. 27–28, pp. 19659–19668, 2020, doi: 10.1007/s11042-020-08847-0.

[30] D. N. H. Thanh, N. H. Hai, V. B. S. Prasath, L. M. Hieu, and J. M. R. S. Tavares, "A two-stage filter for high density salt and pepper denoising," Multimed. Tools Appl., vol. 79, no. 29–30, pp. 21013–21035, 2020, doi: 10.1007/s11042-020-08887-6.

[31] N. Sharma, P. J. S. Sohi, B. Garg, and K. V. Arya, "A novel multilayer decision based iterative filter for removal of salt and pepper noise," Multimed. Tools Appl., vol. 80, no. 17, pp. 26531–26545, 2021, doi: 10.1007/s11042-021-10958-1.

[32] M. B. Ebrahimi, Saviz and Setoudeh, Farbod and Tavakoli, "A New hybrid Method for Noise Robust Estimation of Image Fractal Dimension," Majlesi J. Electr. Eng., vol. 14, no. 2, pp. 25--34, 2020.

[33] Jani, Md & Islam, Md. (2018). De-noising and Feature Extraction of ECG and EEG Signal Using Adaptive Algorithm and Wavelet Transform. 41. 43-56.

[34] K. Zhang, W. Zuo and L. Zhang, "FFDNet: Toward a Fast and Flexible Solution for CNN-Based Image Denoising," in IEEE Transactions on Image Processing, vol. 27, no. 9, pp. 4608-4622, Sept. 2018, doi: 10.1109/TIP.2018.2839891.